

THE INFLUENCE OF HEAT TREATMENT ON THE STRUCTURE AND OXIDATION  
BEHAVIOR OF Zr-2.5wt%Nb.

L.V.Ramanathan, I.Costa and W.A.Monteiro,  
Instituto de Pesquisas Energeticas e Nucleares,  
C.P. 11049, Cidade Universitaria,  
05508 São Paulo, Brazil.



ABSTRACT

This paper presents the influence of different heat treatments on the microstructure and isothermal oxidation behavior of Zr-2.5wt%Nb in oxygen. The quenched structure consisted of martensitic  $\alpha'$ . Upon tempering the quenched alloy at 500°C for upto 100 hours,  $\beta_{\text{Nb}}$  precipitated in the matrix, at twin and  $\alpha'$  needle boundaries. At higher tempering temperatures and after longer periods, Nb rich  $\beta_{\text{Zr}}$  also precipitated. Specimens slowly cooled from the  $\beta$  phase showed the least resistance to oxidation. The oxidation behavior also varied with the tempering time and temperature. The increased oxidation rate of specimens tempered at 500°C for 1000 hours or at 600°C, as compared to those tempered at 500°C for shorter times has been attributed to formation of Nb containing oxides on the coalesced Nb rich precipitate and to cracking.

Key words: Zr-2.5wt%Nb, heat treatment, tempering, microstructure, isothermal oxidation, precipitates.

*Rep. 112*  
8th Int. Symp. on zirconium in the nuclear industry  
San Diego, USA, June 1988.

## INTRODUCTION

The use of zirconium and its alloys in the nuclear industry is quite widespread and is mainly due to its low absorption cross section for thermal neutrons and its mechanical properties. The properties of zirconium alloys in general can be controlled by heat treatments and there have been many investigations of phase transformations in zirconium and its alloys.(1,2) The heat treatment used for strengthening Zr-2.5wt%Nb involves quenching from the  $\beta$ -phase field followed by tempering in the  $\alpha$ -Zr +  $\beta$ -Nb phase region ( see figure 1 ). The microstructural changes produced by heat treatment of Zr-2.5wt%Nb have been investigated by many workers.(2,4,5) They observed equiaxed structures upon annealing, Widmanstätten structures upon slow cooling from  $\beta$ -phase and the precipitation of second phase particles in the matrix and at grain boundaries upon tempering quenched specimens. The nature and composition of the precipitates were reported to vary with the tempering conditions.

The corrosion resistance of Zr-2.5wt%Nb in aqueous and gaseous media is sensitive to among other factors, the microstructure, which in turn is influenced by heat treatment. A number of studies have revealed that annealing in the  $(\alpha + \beta)$  phase region, annealing in the  $\beta$ -phase region, slow cooling through the  $(\alpha + \beta)$ -phase region and just quenching of the alloy decrease the corrosion resistance of the alloy.(6-11) Cox (12) and Cowgill and Smeltzer (13) reported slight improvements in the oxidation resistance upon annealing in the  $(\alpha + \beta)$ -phase field as compared to quenching from the  $\beta$ -phase field. A heat treatment sequence consisting of quenching from the  $\beta$ -phase followed by a 24 hour anneal at 500° C has been reported to be ideal in terms

of corrosion resistance. (14) Quenching from the ( $\alpha + \beta$ )-phase field followed by tempering at 550°C with or without intermediate cold work has also been reported to render microstructures most resistant to corrosion. (15) In some other investigations also, changes in corrosion resistance with tempering conditions have been reported. (8,14,16) This study, which forms part of an ongoing programme of investigation of the oxidation/corrosion behavior of Zr-base alloys, was undertaken to extend the work of previous researchers and to throw more light on the influence of heat treatment on the microstructure and consequently on the oxidation behavior of commercial grade Zr-2.5wt%Nb.

#### MATERIALS AND METHODS

The material was a commercial Zr-2.5wt%Nb alloy received as a 2mm thick sheet. (Analyses for impurities are presented in Table I.) Rectangular specimens approximately 5mm x 5mm were cut degreased, sealed in evacuated quartz capsules and given heat treatments shown in Table II. All the specimens, (except those for transmission electron microscopy) were prepared under identical conditions to minimize the influence of surface preparation. Standard metallographic techniques followed by a final etch-polish in a 10% HF, 25% H<sub>2</sub>SO<sub>4</sub>, 30% HNO<sub>3</sub> and balance water solution were used. Specimens for transmission electron microscopy (TEM) were also prepared using standard techniques. (17)

The isothermal oxidation measurements on the annealed, slowly cooled, quenched and quenched-short time tempered specimens were carried out in the temperature range 350-700°C for 400 minutes in a constant flux of oxygen. The specimens tempered for longer times were isothermally oxidized at 600°C for 400 minutes. The scatter in the oxidation data (average of

3 or more measurements) for specimens heat treated in the same batch was very small.

## RESULTS AND DISCUSSION

### Optical Microscopic Observations

The annealed specimen revealed typical equiaxed structure and  $\beta_{Zr}$  at the grain boundaries. Slow cooling from the  $\beta$ -phase resulted in a structure shown in figure 2a. formed by nucleation of  $\alpha$ -Zr at the  $\beta$  grain boundaries and its subsequent growth to form a Widmanstätten structure. Upon quenching from the  $\beta$ -phase,  $\beta$  transforms to martensitic  $\alpha'$  as shown in figure 2b. The structure of the specimen tempered at 500° C for 10 hours revealed both rounded and slightly elongated precipitates in a martensitic matrix of  $\alpha'$ . (Figure 2c) The precipitates increased in size but decreased in number with increasing tempering time and were found to be  $\beta_{Nb}$  (determined by selected area diffraction -SAD in the TEM). The specimen tempered at 550° C for 10 hours revealed fewer but larger  $\beta_{Nb}$  precipitates. Prolonged tempering at 550° C resulted in a structure shown in figure 2d.

### Transmission Electron Microscopic Observations

The structure of the quenched specimen was characterized by internally twinned martensitic  $\alpha'$  needles. The structure of the specimen tempered at 500° C for 10 hours revealed  $\beta_{Nb}$  precipitates at the  $\alpha'$  needle boundaries (see figure 3a), at microtwin boundaries and associated with matrix dislocations. After longer times at 500° C, very fine aligned precipitates within the matrix were also observed as shown in figure 3b. Upon tempering at 550° C and 600° C the average precipitate size increased and were present predominantly at  $\alpha'$  needle boundaries.

A large number of aligned precipitates at pre-existing twin boundaries were also observed as shown in figure 3c and found by SAD analysis to be niobium rich  $\beta_{\text{Nb}}$ . Prolonged tempering at 550° C and 600° C led to growth of transformed  $\beta_{\text{Zr}}$ . Similar observations have been reported by Bannerjee et.al.(18) Polygonization has also been observed upon tempering at 600° C as shown in figure 3d. Overall, with increasing tempering temperature and time, a change in the nature and composition of the precipitate has been observed as summarized in Table III.

#### Oxidation Measurements

The results of the isothermal oxidation studies carried out at 350-700° C with specimens in the different heat treated conditions are shown in figure 4. At all temperatures, the annealed specimens exhibited the highest resistance and the specimens slowly cooled from the  $\beta$ -phase field, the lowest oxidation resistance as compared to specimens given other heat treatments. The oxidation behavior of the quenched as well as the low temperature short time tempered specimens were similar. However the quenched specimens oxidized to a slightly greater extent than the tempered specimens at all temperatures. Similar observations have been reported by Klepfer(9) and Daalgard(14) for alloys quenched and slowly cooled from the  $\beta$ -phase.

The results of the isothermal oxidation measurements carried out at 600° C with the long term tempered specimens are summarized in figures 5 and 6. The higher extent of oxidation of specimens tempered for 10 hours at 500° C as compared to those tempered for 100 hours at the same temperature can be attributed to the presence of large quantities of Nb rich  $\alpha'$  in the former

and a more even distribution of fine  $\beta_{\text{Nb}}$  in the latter. Similar observations were made by Cox(16) who found the oxidation rate at 300°C in moist air to decrease with increasing tempering time upto 168 hours. The oxidation behavior of specimens tempered at 550°C and 600°C is different. The specimens tempered for 1000 hours oxidize more than those tempered for 10 or 100 hours. Morphological examination of oxidized specimens tempered at the higher temperatures for longer times revealed regions with thicker oxide. These thick oxide regions corresponded to coalesced precipitates(17). The formation of similar thick oxide spots on  $\beta_{\text{Nb}}$  precipitates after prolonged oxidation of Zr-2.5wt%Nb have been reported and attributed to the probable transfer of Nb into the oxide and the subsequent change in stoichiometry of the oxide(12). Cracks in the oxide at the  $\alpha/\alpha'$  interface have also been observed (13,17) as shown in figure 5. Thus the change in the oxidation behavior of specimens tempered at higher temperatures as compared to those tempered at 500°C is due to both the presence of the large coalesced precipitates which oxidize at a higher rate than its surrounding  $\alpha'$  or  $\alpha$ -Zr and also to oxide cracking.

#### CONCLUSIONS

1. Slow cooling of Zr-2.5wt%Nb from the  $\beta$ -phase field gives rise to microstructures revealing large precipitates, some of which are found located at grain boundaries. This type of microstructure has been found to be related to low oxidation resistance.
2. Upon tempering quenched alloy at 500°C, depending on the tempering time, precipitation of  $\beta_{\text{Nb}}$  occurs in the matrix, at  $\alpha'$  grain boundaries and at twin boundaries. After longer times and at higher temperatures  $\beta_{\text{Zr}}$  also precipitates and the precipitates coalesce.

3. The oxidation behavior at all temperatures varies with the heat treatment. Annealed specimens showed maximum resistance where as specimens slowly cooled from the  $\beta$ -phase the least. Tempering of the quenched specimen at 500° C increases oxidation resistance.
4. Oxidation behavior of the long term tempered specimens are influenced by the nature, distribution and size of the precipitates. Low  $\alpha'$  content and even distribution of  $\beta_{\text{Nb}}$  precipitates contribute to increasing the oxidation resistance of specimens tempered at 500° C for upto 100 hours.
5. The lowered oxidation resistance of specimens tempered for long periods at 550° C and 600° C is due to the coalesced precipitates over which Nb rich oxides are thought to form, which increase in volume and lead to cracking at the thick/thin oxide boundary.

#### REFERENCES

1. Douglas, D.L., Atomic Energy Review, Supplement 1971, International Atomic Energy Agency, Vienna, 464, 1971.
2. Northwood, D.O. and Lim, D.T., Canadian Metallurgical Quarterly, Oct-Dec., 18(21), 441, 1979.
3. Lundin, C.E. and Cox, R.H., Proc. USAEC symp. Zr. Alloy Develop., Pleasonton, California, Nov. 1962, GEAP-4089. vol. 1, 9.1, (1962).
4. Aldridge, S.A. and Cheadle, B.A., Journal of Nuclear Materials 42, 32, 1972.
5. Shemyakin, V.N. and Bainova, G.D., Fiz. Met. Metalloved, 60(4), 827, 1985.
6. Cox, B., Advances in Corrosion Science and Technology, vol. 5, (Ed) Fontana, M.G. and Staehle, R.M., Plenum Press, 173, 1976.

7. Parfenov, B.G., Gerasimov, V.V., Venediktova, G.I., Corrosion of zirconium and zirconium alloys, Moskva, Atomizdat, 34, 1967.
8. Anderko, K., Jung-Konig, W., Richter, H., Schleicher, H.W. and Zweiker, U., Zeitschrift fur Metallkunde, 53, 503, 1962.
9. Klepfer, H.H., Journal of Nuclear Materials 9, 65, 1963.
10. Lesurf J.E., The Corrosion Behavior of 2.5%Nb zirconium alloy, Proc. ASTM symp. Applications related to phenomenon in Zr and its alloys, Philadelphia, ASTM-STP 458, 1968.
11. Lees, D.G., Corrosion Science, 5, 565, 1965.
12. Cox, B., Long term oxidation of Zr-2.5wt%Nb alloy, AECL-5610, Chalk River Nuclear Laboratories, Chalk River, Ontario, Canada, 1976.
13. Cowgill, M.G. and Smeltzer, W.W., Journal of Electrochem. Soc., vol. 114, 11, 1967.
14. Dalgaard, S.B., Corrosion of reactor Materials. vol. 2, IAEA conference, IAEA, Vienna, 159, 1962.
15. Evans, E.N. and Lees, D.G., U.K. Patent 988069, 1963.
16. Cox, B. and Read, J.A., UKAEA Report AERE-R 4459, 1963.
17. Costa, I. and Ramanathan, L.V., submitted for publication in CORROSION journal.
18. Banerjee, S., Vijay Kumar, S.J. and Krishnan, R., Journal of Nuclear Materials, 62, 229, 1976.

TABLE I. Analyses of impurity content of Zr-2.5wt%Nb.

Element	ppm(max)	Element	ppm(max)
Al	41	Mo	<25
B	0.2	N	37
C	120	Ni	<35
Cd	<0.2	O	1010
Co	<10	Pb	<50
Cr	<50	Si	43
Cu	25	Sn	<10
Fe	457	Ta	<200
H	<5	Ti	<40
Hf	26	U	1.2
Mg	<10	V	<25
Mn	<25	W	<25

TABLE II. Summary of Heat Treatments given to Zr-2.5wt%Nb

Heat treatment	Conditions		
Annealing	500° C for 1 hour.		
Quenching	1100° C for 1 hour followed by quenching in water.		
Slow cooling	1100° C for 1 hour followed by furnace cooling.		
Tempering	Quenching followed by annealing at (hours)		
	500° C	550° C	600° C
	4	-	-
	10	10	10
	100	100	100
	1000	1000	1000

TABLE III. Summary of phases and precipitates present in tempered Zr-2.5wt%Nb.

Tempering time (hours)	Tempering temperature (°C)		
	500	550	600
10	$\alpha' + \beta_{\text{Nb}}$	$\alpha' + \beta_{\text{Nb}} + \beta_{\text{Zr}}$	$\alpha' + \beta_{\text{Nb}} + \beta_{\text{Zr}}$
100	$\alpha' + \beta_{\text{Nb}}$	$\alpha + \beta_{\text{Zr}}$	$\alpha + \beta_{\text{Zr}}$
1000	$\alpha' + \beta_{\text{Nb}} + \beta_{\text{Zr}}$	$\alpha + \beta_{\text{Zr}}$	$\alpha + \beta_{\text{Zr}}$

LIST OF LEGENDS.

Figure 1. Equilibrium phase diagram of the Zr-Nb system.(3)

Figure 2. Optical micrographs of Zr-2.5wt%Nb:

- (a) slowly cooled from  $\beta$ -phase. 600X;
- (b) quenched from  $\beta$ -phase, 300X;
- (c) tempered at 500° C for 10 hours, 400X;
- (d) tempered at 550° C for 1000 hours, 400X.

Figure 3. Transmission electron micrographs of Zr-2.5wt%Nb alloy tempered at:

- (a) 500° C for 10 hours, 55000X;
- (b) 500° C for 1000 hours, 35000X;
- (c) 600° C for 100 hours, 40000X;
- (d) 600° C for 1000 hours, 20000X.

Figure 4. Influence of heat treatment on oxidation behavior of Zr-2.5wt%Nb in oxygen at (a) 350° C, 400° C; (b) 500° C; (c) 700° C.

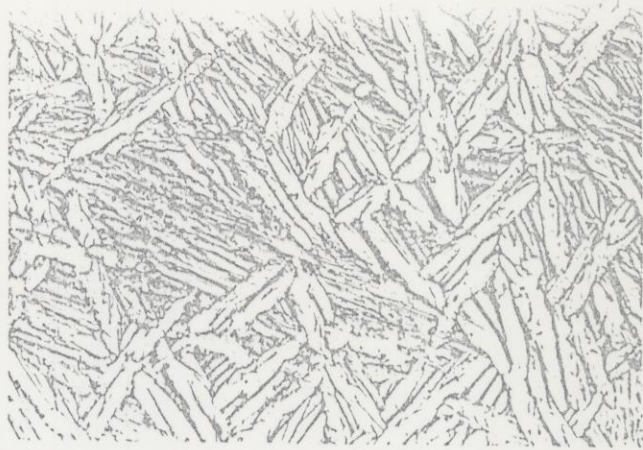
Figure 5. Isothermal weight gain curves at 600° C in oxygen for Zr-2.5wt%Nb tempered at (a) 500° C, (b) 550° C, (c) 600° C.

Figure 6. Weight gain of tempered Zr-2.5wt%Nb at 600° C over 400 minutes versus tempering time.

Figure 7. Scanning electron micrograph of oxide surface on Zr-2.5wt%Nb tempered at 600° C for 1000 hours. 3000X.

Fig. 2

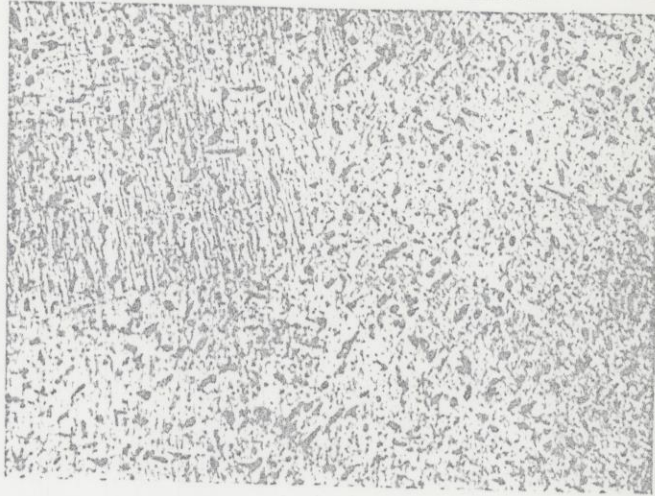
(a)



(b)



(c)



(d)

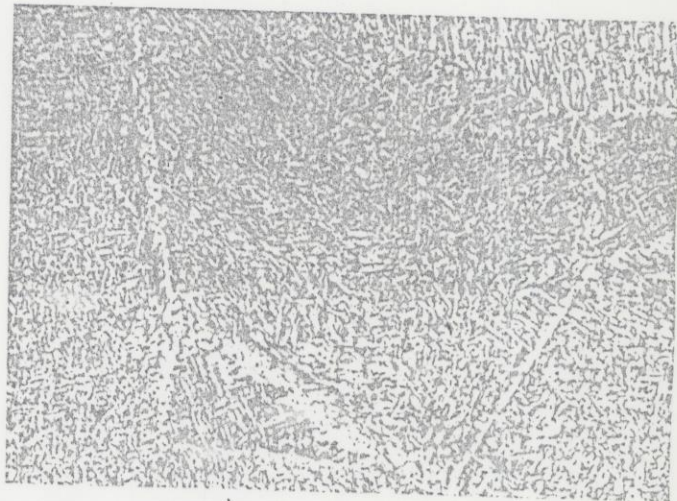




FIG. 3a



FIG. 3b



FIG. 3c



FIG. 3d.



FIG. 7

Fig. 1

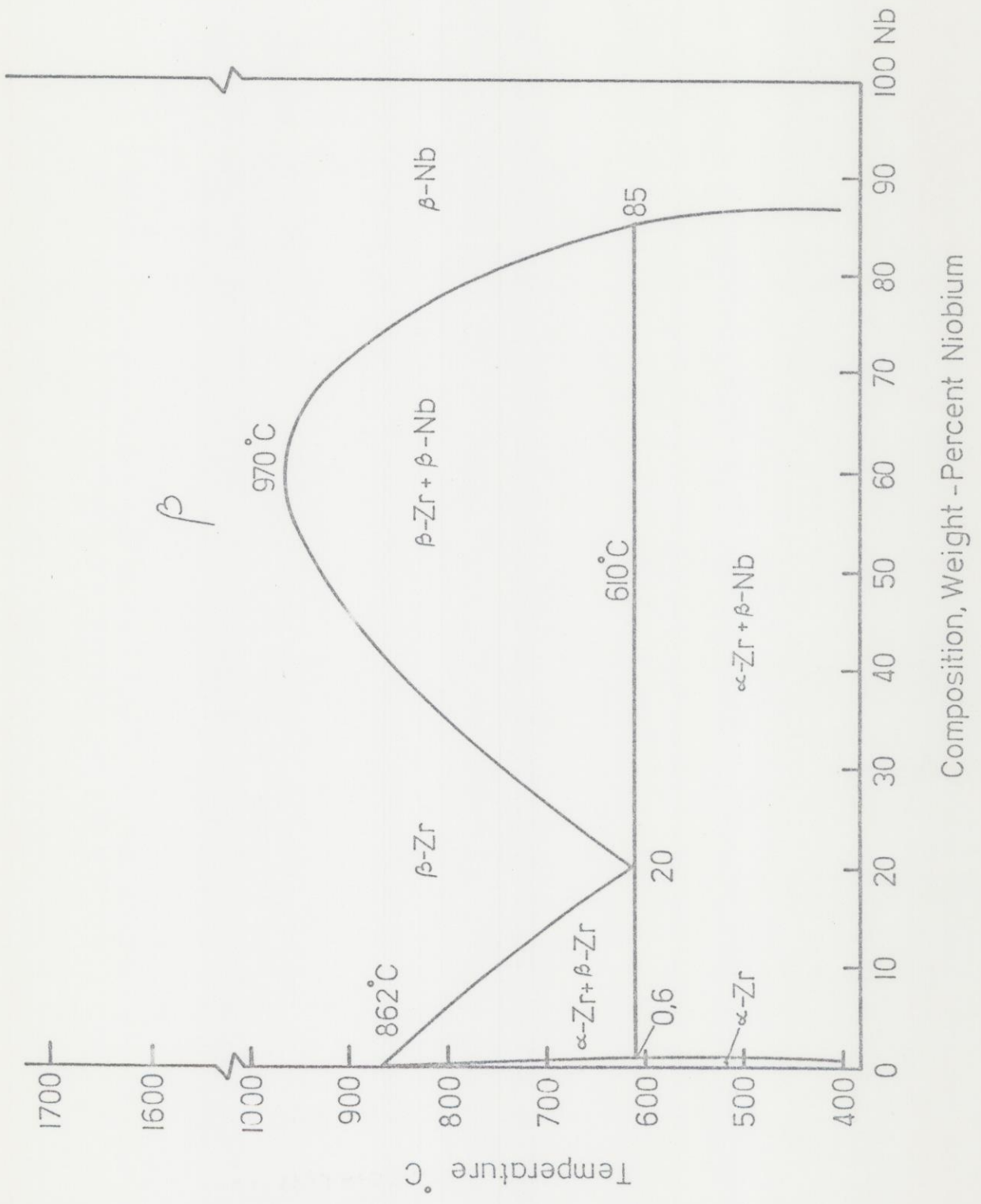


FIG. 4(9)

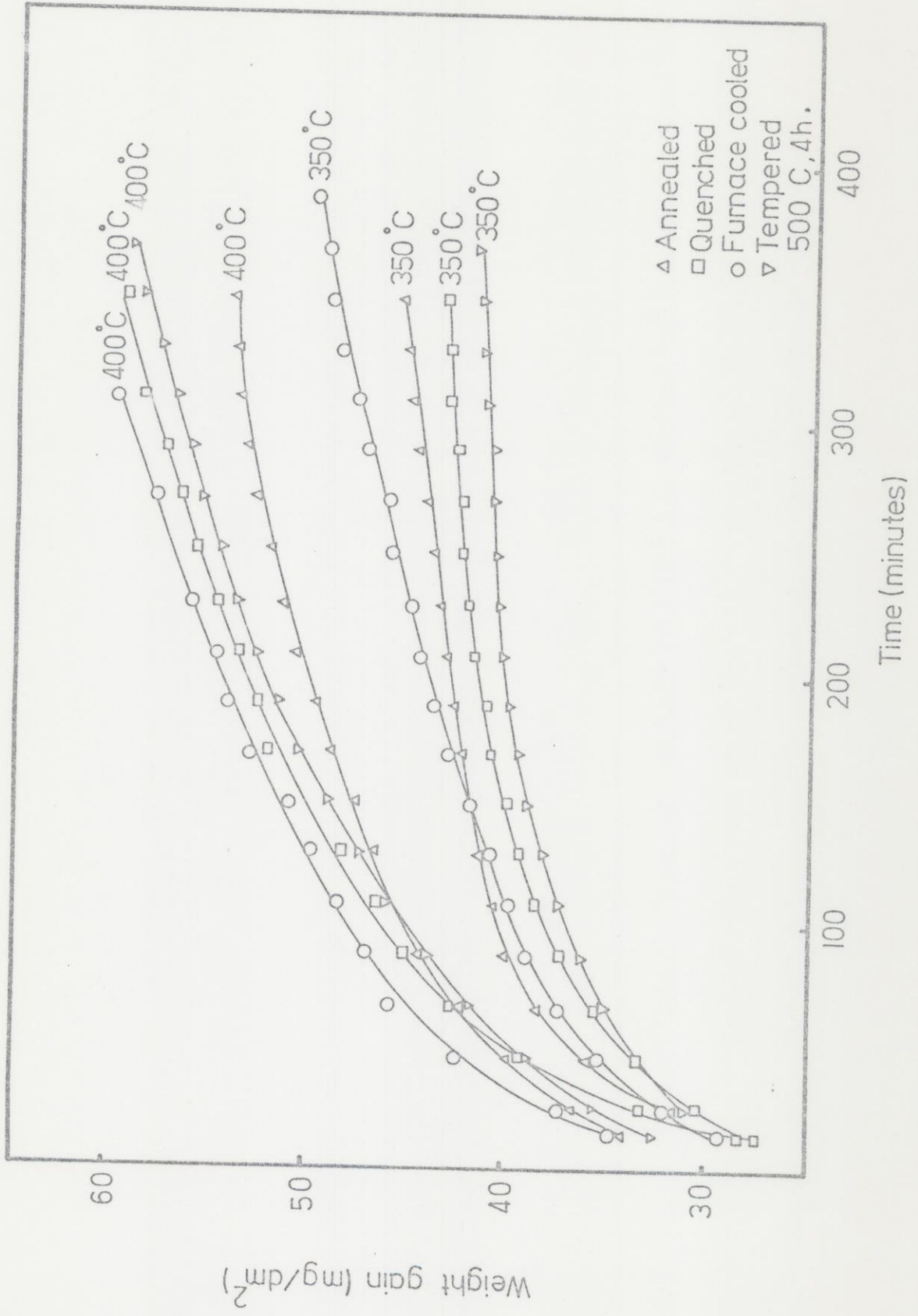


Fig. 4(b)

FIG. 4b.

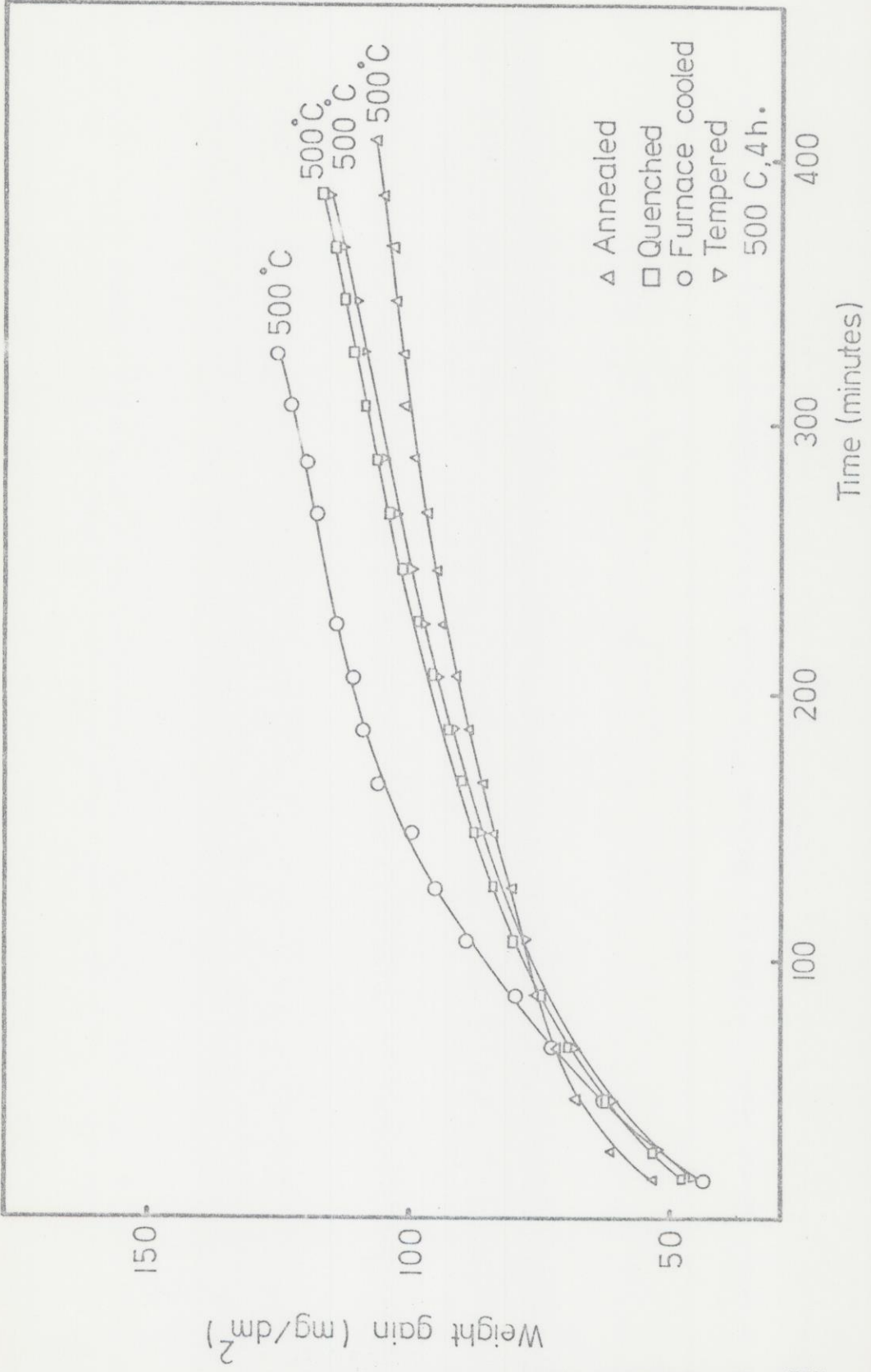
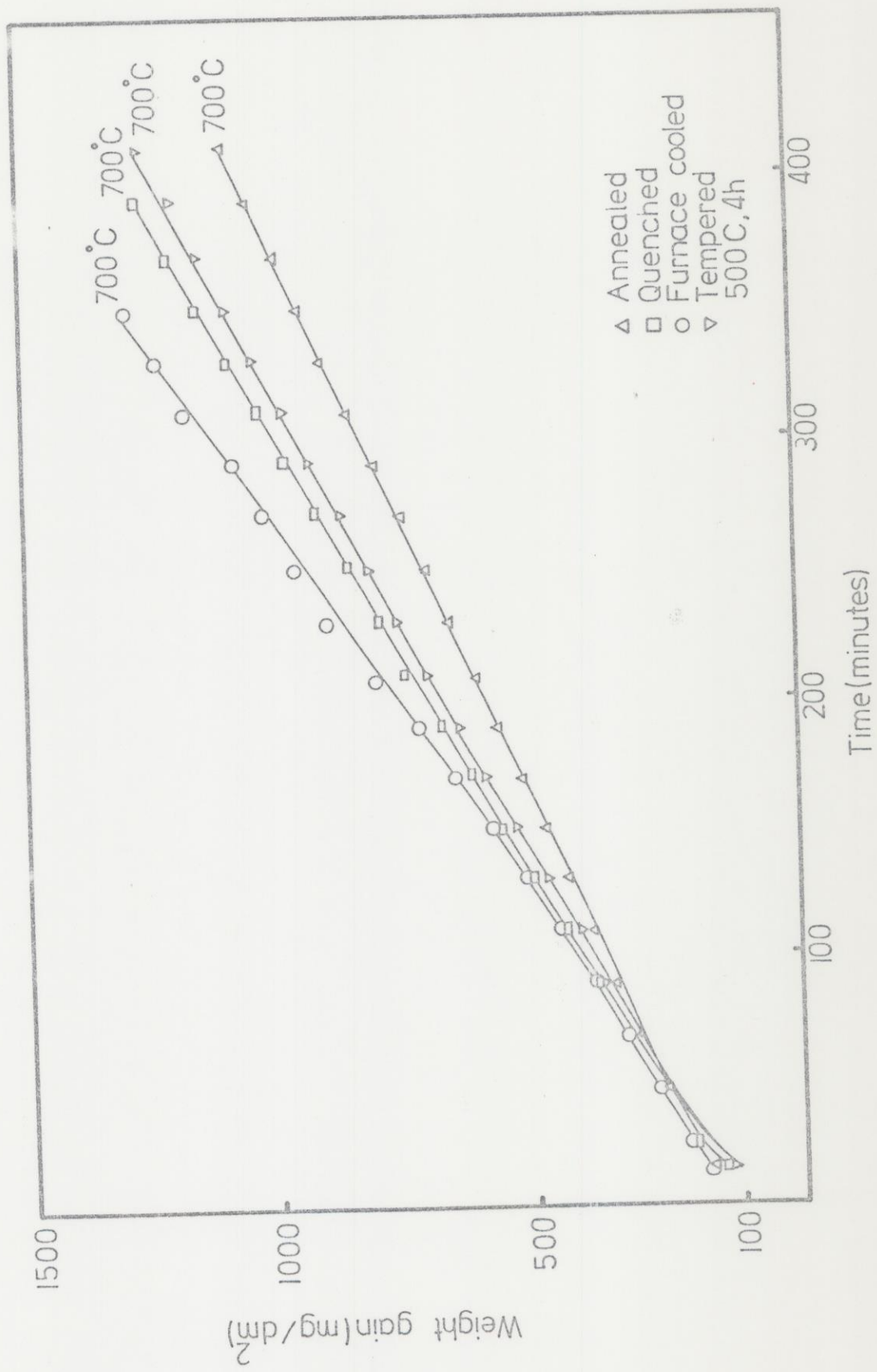


Figure 4c

FIG. 4c



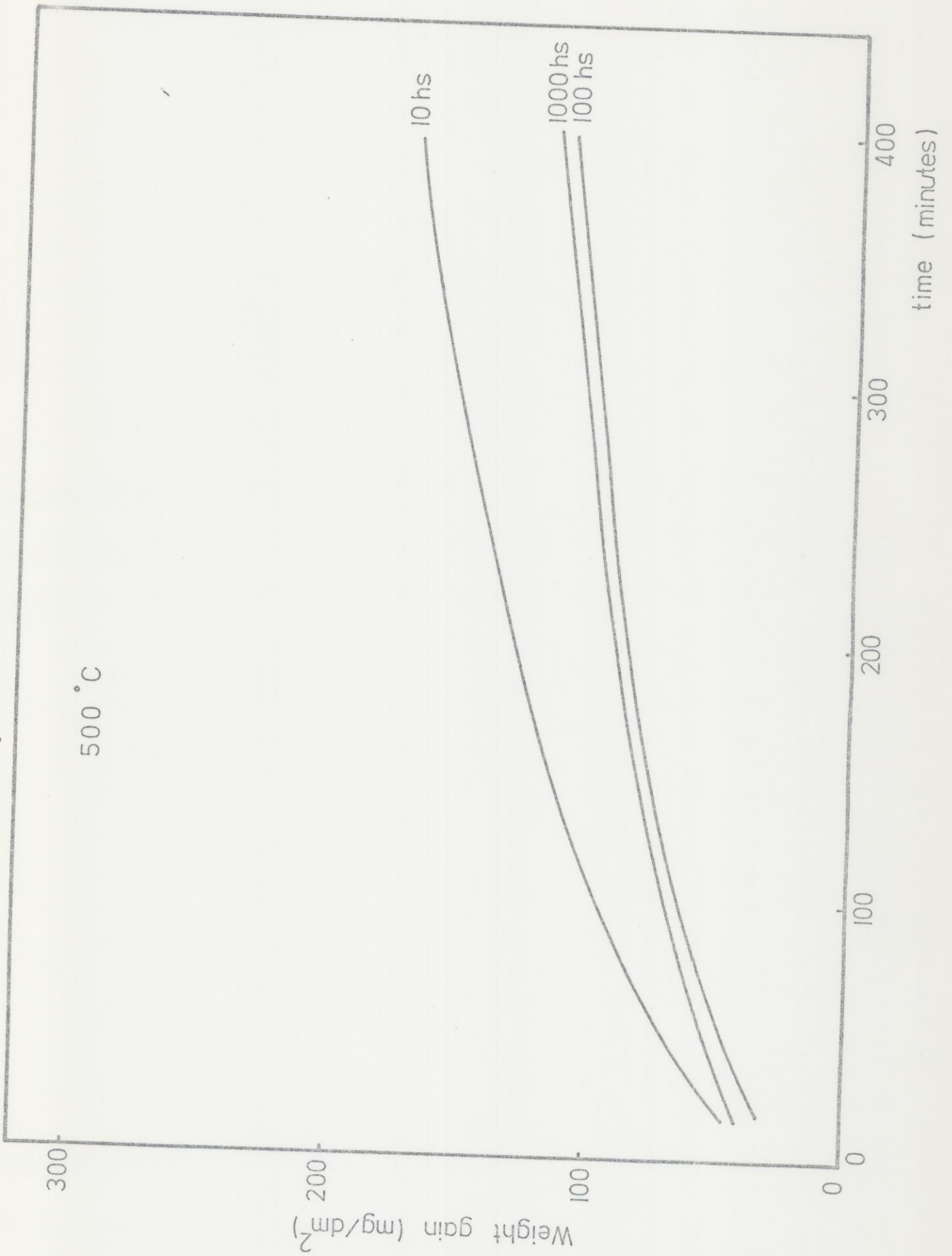


FIG. 59.

Figure 59

Fig. 5b

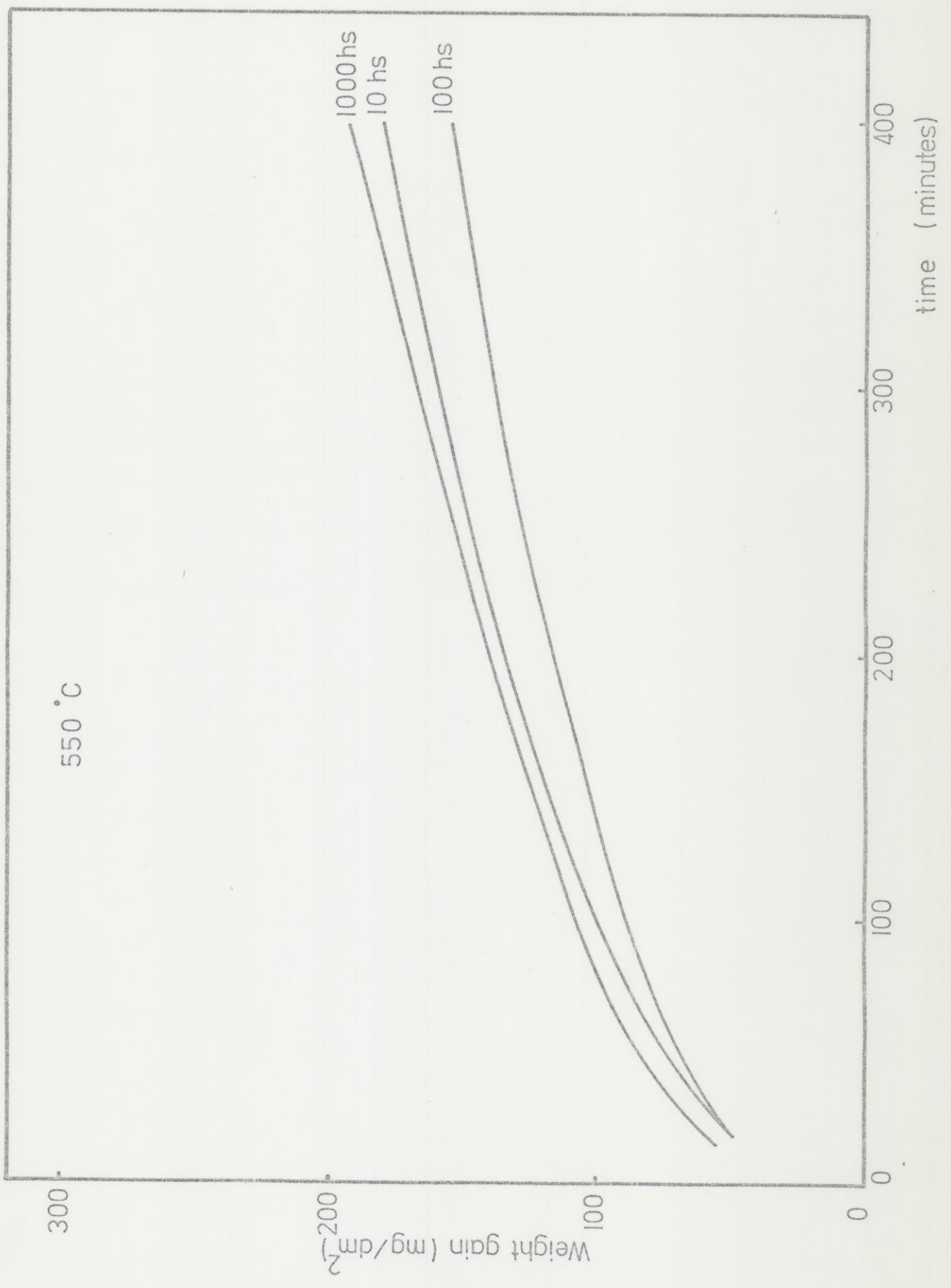


Fig. 5c



Fig. 6

